Research Papers

CENTRO EURO-MEDITERRANEO
PER I CAMBIAMENTI CLIMATICI

ISC – Impatti sul Suolo e sulle Coste

Effects of the climatic conditions on the behaviour of a slow landslide in clay

Luca Comegna, PhD
Centro euro-Mediterraneo per i Cambiamenti Climatici, CMCC

Centro Euro-Mediterraneo
per i Cambiamenti Climatici
www.cmcc.it

December 2009 ■ RP0095

Effects of the climatic conditions on the behaviour of a slow landslide in clay

Summary
This report contains the results of some numerical simulations performed in order to furnish a methodological approach aimed to understand the influence of the climatic conditions on the behaviour of a slow earthflow. The analyses have been performed using the numerical model adopted by the FEM code VADOSE/W (Krahn, 2004), which allows to assess the interaction existing between the ground surface of a soil deposit and the atmosphere due to the alternating climatic conditions.
Moreover, a scenario of the long-time future behaviour has been estimated thanks to the results coming from the analyses performed by the COSMO-CLM climatic model.

Keywords: numerical simulation**,** slow landslide, clay, climatic conditions.

JEL Classification:

Address for correspondence:
Luca Comegna
PhD in Geotechnical Engineering
Seconda Università degli studi di Napoli
Department of Civil Engineering
Via Roma, 29
81031 Aversa (CE)
E-mail: luca.comegna@unina2.it

CONTENTS

1. Foreword

Some numerical analyses have been performed in order to reproduce the effects of the climatic conditions on the piezometric course monitored within the body of a very slow landslide involving fine-grained soils. This aspect is relevant because the periodicity of the weather gives quite a regular course to the piezometric levels, which fluctuate between minimum and maximum values, so influencing the behaviour of the landslide and, in particular, its velocity.
The adopted approach is characterized by a 1D modelling of the seepage and evaporation processes through the deposit as a consequence of the external climate data imposed as ground surface boundary condition.
In order to define a potential long term scenario, we have also taken into account the results coming from some analyses aimed to outline long-term future climatic trends and performed by the climatological division of C.I.R.A. through the use of COSMO-CLM climatic model.

2. The examined test case

2.1Monitoring data

The analyses regard the case of an earthflow in Varicoloured Clays which interest an about 10° inclined slope, set inside a zone located in the eastern part of the urban area of Potenza (Southern Italy). The landslide body (Fig. 2.1) is about 1650 m long and spreads between the altitudes 900 m and 620 m a.s.l.. Its accumulation zone invaded the bed of the downslope Basento River.

Figure 2.1. The analysed landslide

The landslide is now characterized by a very low velocity (about 1÷2 cm/year), so that according to Cruden and Varnes (1996), the earthflow is now classifiable as very slow. As known, because of the low hydraulic conductivity of the involved soils, the activity of

similar landslides is generally not influenced by single intense rainy events (the infiltrability is low) but, on the contrary, is normally governed by the rainfall that cumulate over long time periods (about some months).
The available monitoring data regard information about:
- displacements;
- pore-water pressures;
- climatic data.

The displacements and pore-water pressures data have been derived from the works published by Vassallo and Di Maio in 2006, 2007 and 2008. In particular, the displacements data regard the values measured by an inclinometer, reported as I3 in Figure 2.1, installed within the track of the earthflow, while the pore-water pressures data regard the piezometric levels measured by a Casagrande piezometer, named S1 in Figure 2.1, and installed within the accumulation zone of the landslide.
The inclinometer furnishes information about displacements from 15/03/2005 to 13/07/2006, while piezometric data are available from 11/01/2005 to 23/05/2008.
The presence of a slip surface within the track of the landslide has been recognised by I3 at the depth of about 9 m from the ground surface. Figure 2.2 shows the displacements cumulated at the slip surface during that period and the relative velocities: as a matter of fact, it is evident that the rate of displacement tends to grow in correspondence of high piezometric levels. In particular, an acceleration phase of the landslide body is rather evident from 09/12/2005 to 21/03/2006: during that period, the average rate of displacement is about 0.3 cm/month, instead of 0.1 cm/month shown before and after that time interval.
In order to create a relationship between rates and pore-water pressures, we have used the following power law

$$v = \frac{a}{h^b} \qquad [2.1]$$

where v [cm/day] is the velocity, h [m] is the piezometric level (i.e. the difference between the installation depth and the measured pressure head), a and b are back analysed calibrating parameters. With regard to this topic, we have taken into account the hysteretic behaviour observed for similar landslides by Bertini et al. (1986), who stated that the rate of movement is higher if a determined piezometric level is attained during an increasing phase of the groundwater rather than during its decreasing phase. Therefore, the following parameters:

- a = 0.0100, b = 1 (during increasing pore-water pressure phases)

- a = 0.0708, b = 1 (during decreasing pore-water pressure phases)

have furnished the calculated curve reported in Figure 2.3, that reproduces rather satisfactorily the measured values.

The available measured climate data regard:
- daily rainfall, from 1916 to 2007, reported by the hydrological annals and relative to a pluviometric station set at an altitude equal to 811 m a.s.l.;

- rainfall, air temperature and relative humidity data registered every 20 minutes, from 01/01/2005 until 31/12/2007, by a station installed by ARPAB (Agenzia Regionale per la Protezione dell'Ambiente della Basilicata) at an altitude equal to 659 m a.s.l..

Both the stations are located not so far from the site (about 7.50 Km).
Regarding to these data, it's interesting to note that, as reported by Figure 2.4, during the last century the yearly cumulated rainfall show a general decreasing trend. Moreover, Figure 2.5 shows the course of the daily maximum and minimum value of air temperature and relative humidity from 2005 to 2007: it's evident that during summer months air temperature and relative humidity attain respectively their maximum and minimum values.

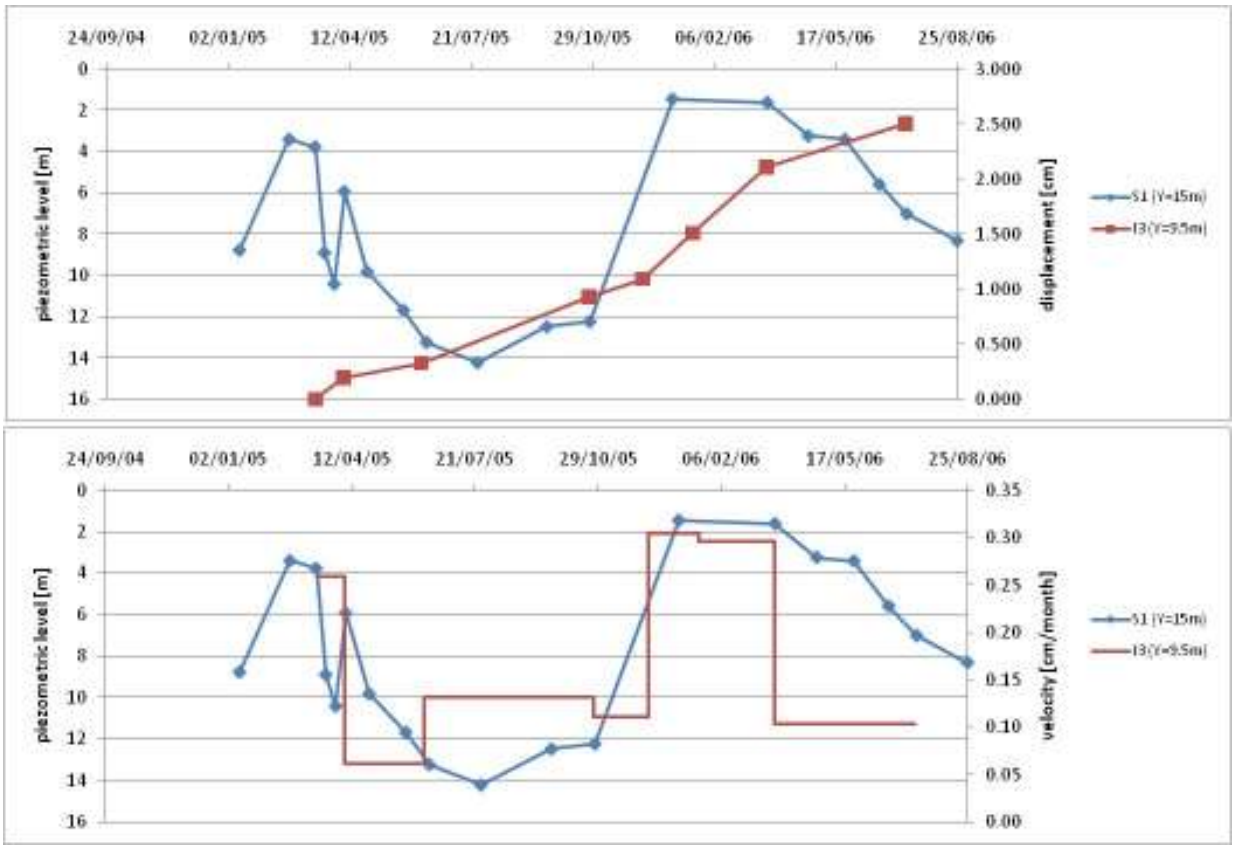

Figure 2.2. Cumulated displacements measured at the slip surface within the track and relative velocities compared with piezometric levels

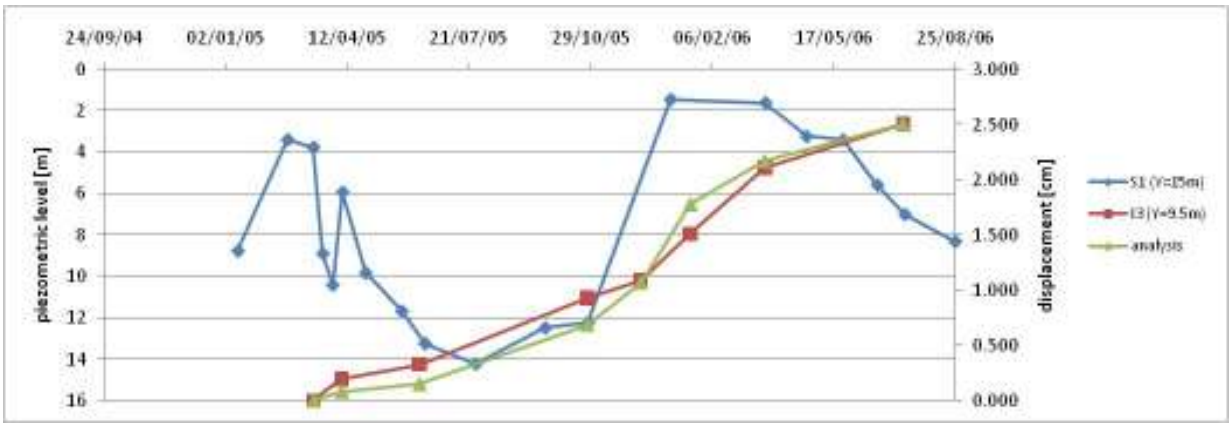

Figure 2.3. Measured displacements compared with simulated displacements

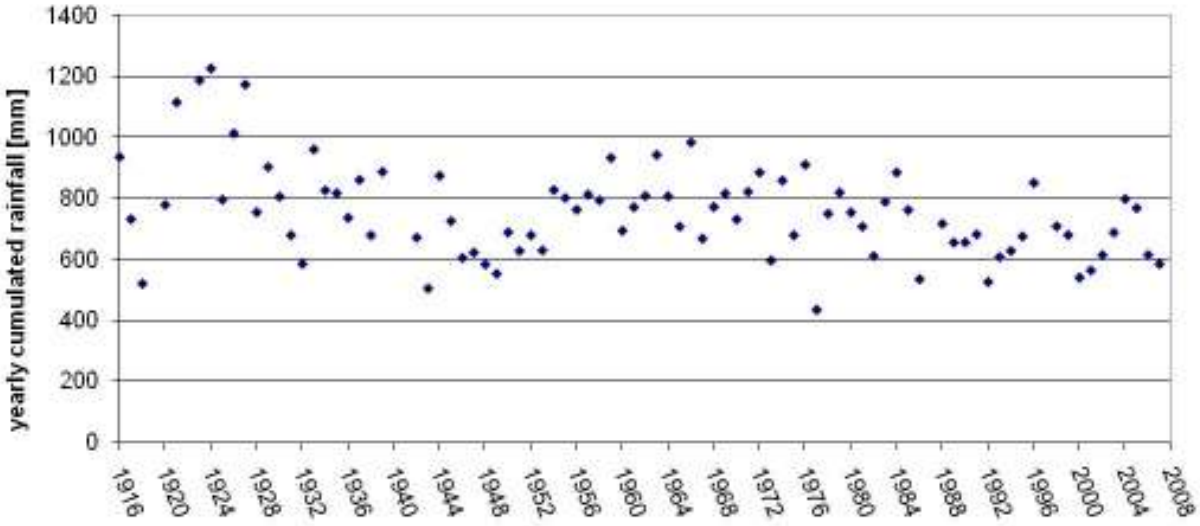

Figure 2.4. Yearly cumulated rainfall measured from 1916 to 2007

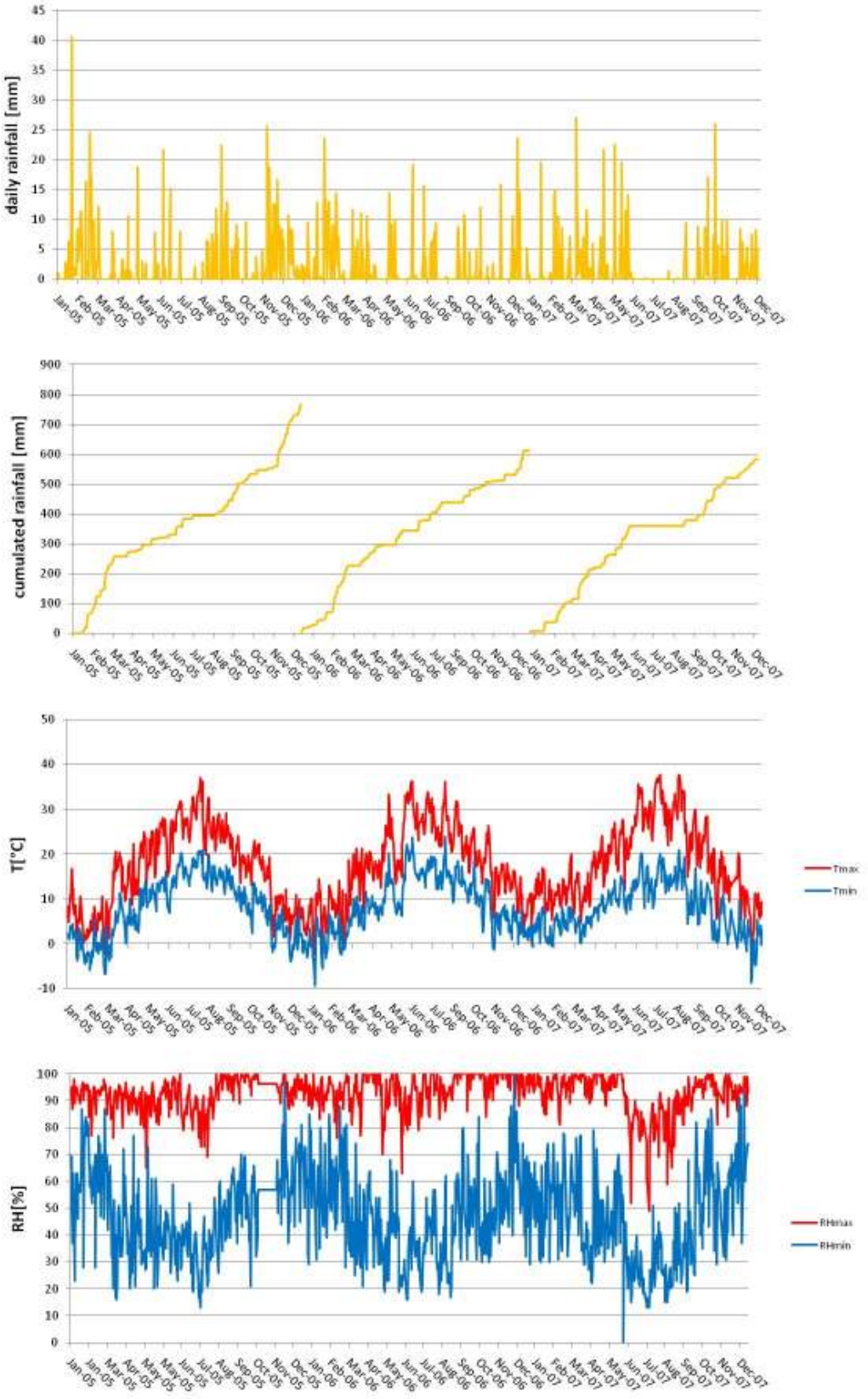

Figure 2.5. Rainfall, maximum and minimum values of temperature T and relative humidity RH measured from 01/01/2005 to 31/12/2007

2.2 Calculated climate data

The climatological task of C.I.R.A. has performed some analyses through the use of the COSMO-CLM climatic model, which have been directed to furnish future climatic scenarios of the interested area. In particular, the extracted output data which have been considered useful to the seepage analyses have regarded daily information about

- rainfall;
- maximum and minimum temperature;
- maximum and minimum relative humidity;
- average wind speed

during the time interval 2005-2060.

As regard the yearly cumulated rainfall data, from a comparison between the calculated and measured values, which is possible only from 2005 to 2007, we have noted not so many differences. In fact, the measured values are 766, 612 and 582 mm, respectively attained in 2005, 2006 and 2007, while the corresponding calculated values are 788, 653 and 707 mm (Fig. 2.6). At the same time, the decreasing future trend showed by the calculated yearly rainfall until 2060 (gradient of about -1.80 mm/year) seems to agree with the measured one until 2007 (Fig. 2.7). On the other hand, the daily data are very different, in fact the cumulated rainfall calculated during the mentioned three-year period spread along a total number of days (165) that is about the 40% of the real one (392). This is due to a calculated distribution, characterized by days with sudden rainy peaks spaced out by a large number of no rainy days (Fig. 2.8b), which doesn't reflect the monitored one (Fig. 2.8a).

We have also compared the calculated values of temperature (Fig. 2.9) and relative humidity (Fig. 2.10), with the monitored ones from 2005 to 2007. Regarding the temperature, we have noted that the calculated maximum and minimum values are respectively 2°C and 9°C (Fig. 2.11) higher on average with respect to the measured, but show a very similar course. At the same time, the calculated maximum and minimum values of relative humidity (Fig. 2.12) are respectively 23% lower and 10% higher on average than the corresponding measures, but show again quite a similar path.

Finally, Figure 2.13 shows the calculated values of wind speed. Unfortunately, those values can't be compared with the corresponding measured values, because of the absence of relative monitoring information.

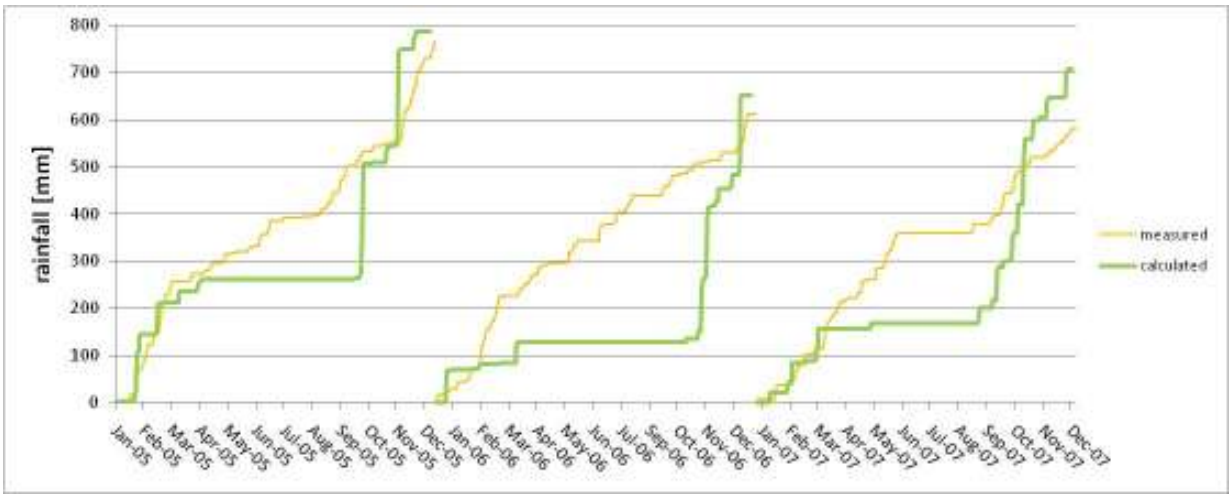

Figure 2.6. Measured and calculated cumulated rainfall from 2005 to 2007

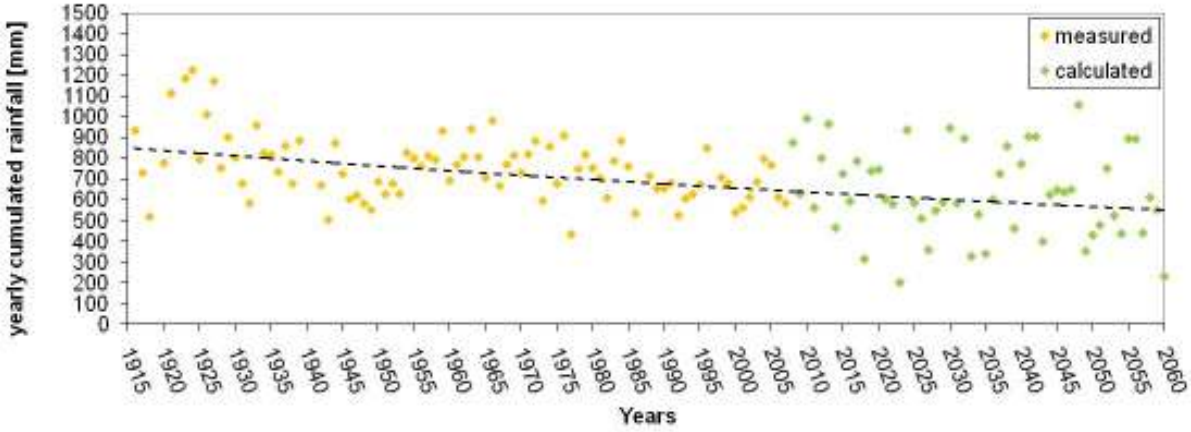

Figure 2.7. Measured and calculated yearly cumulated rainfall

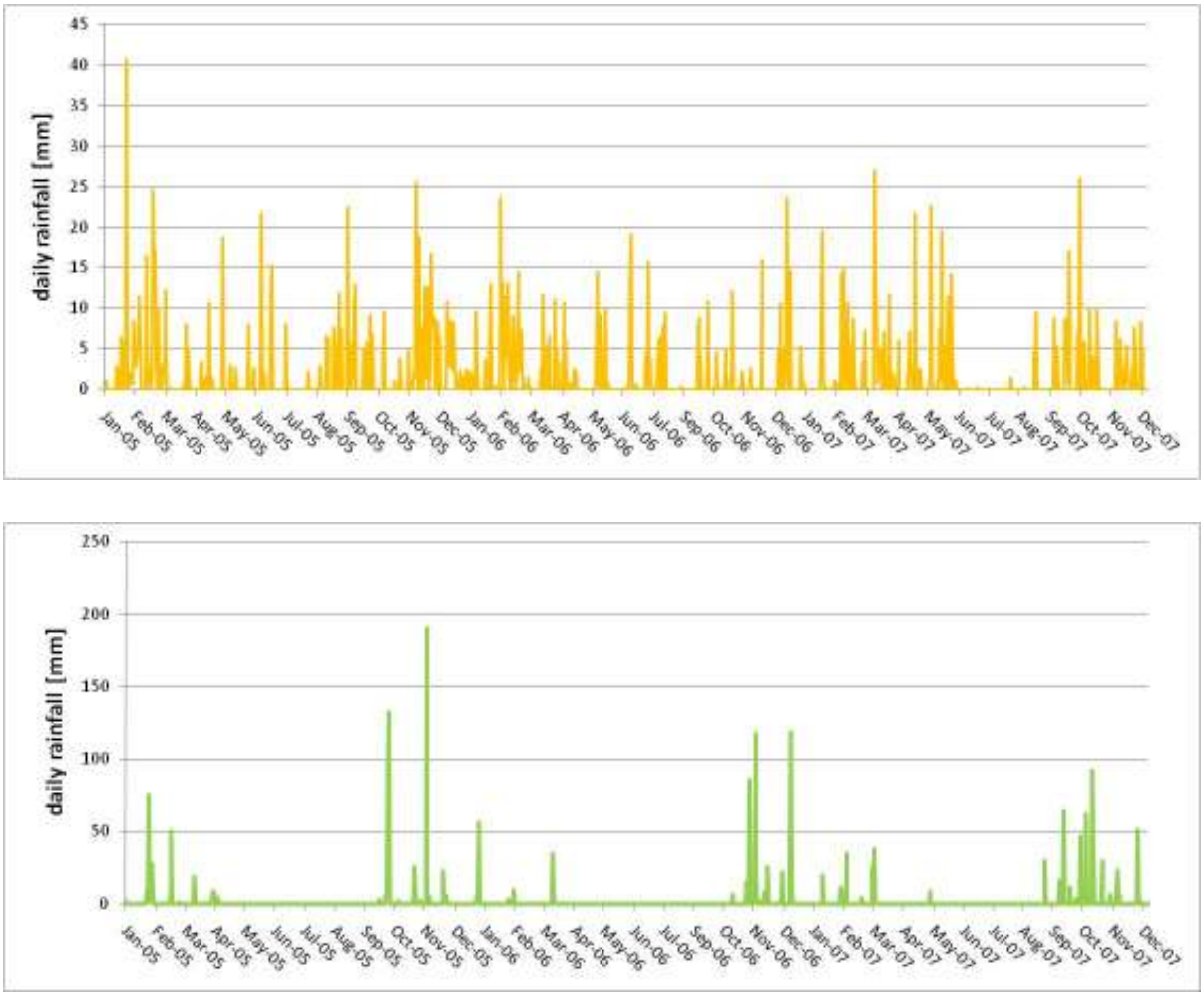

Figure 2.8. Measured (a) and calculated (b) daily rainfall from 2005 to 2007

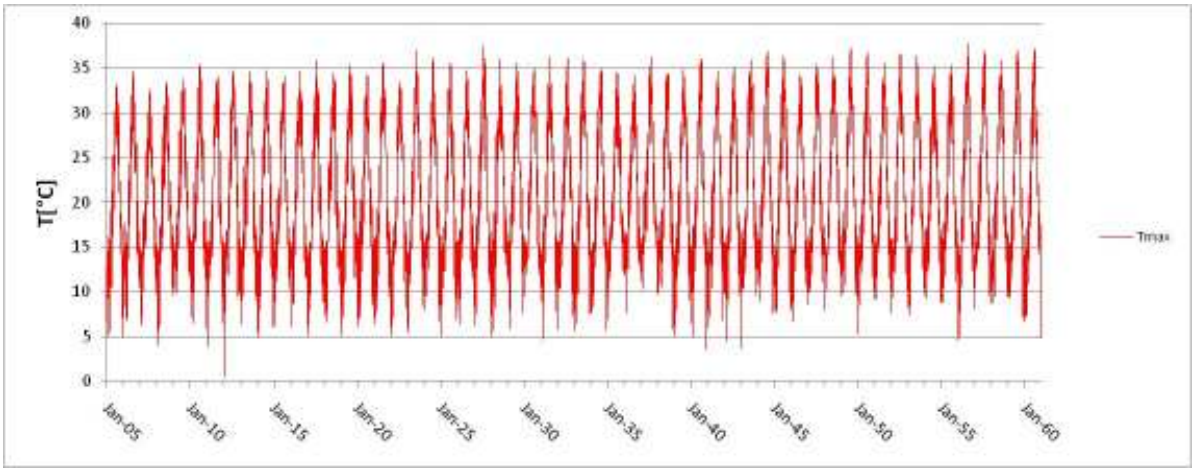

a)

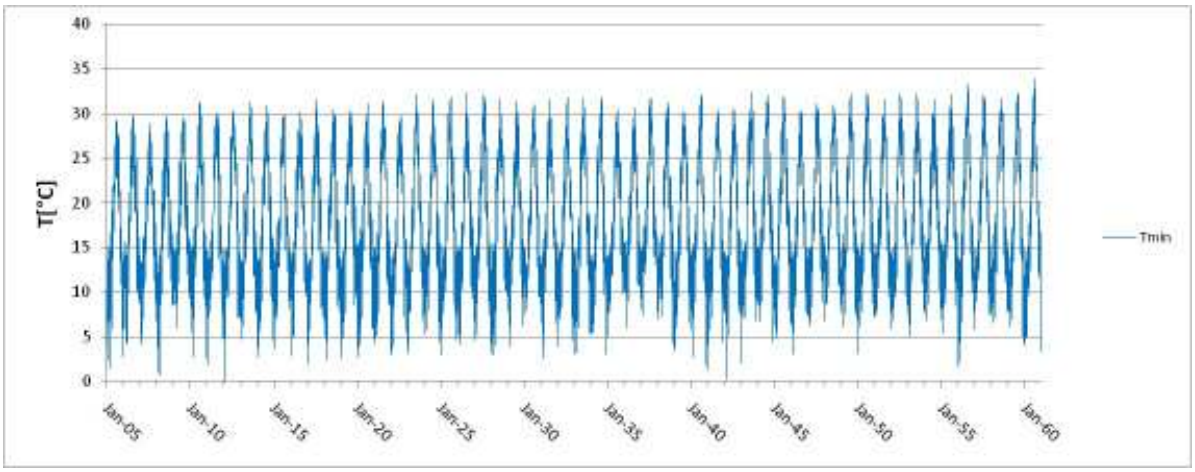

b)

Figure 2.9. Calculated daily maximum (a) and minimum (b) values of temperature

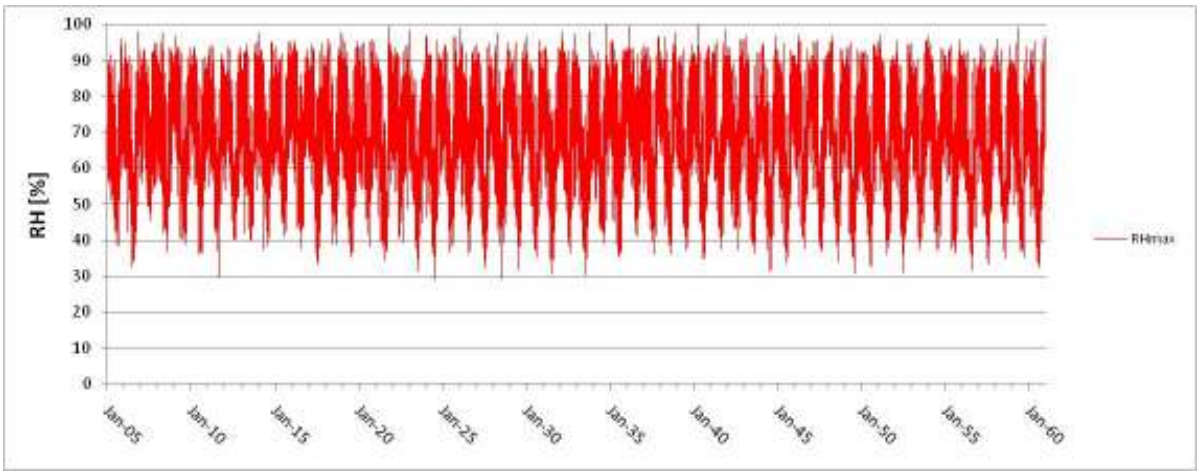

a)

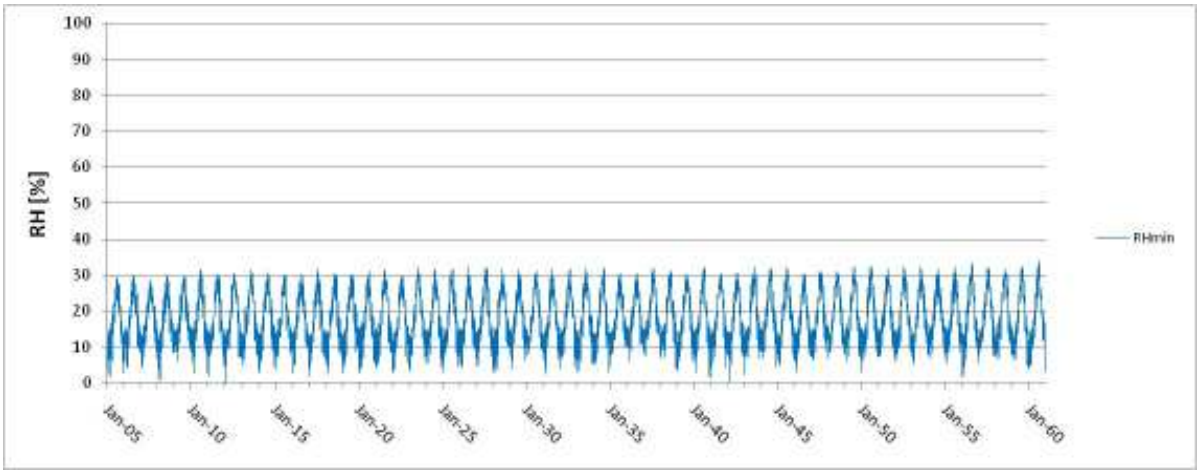

b)

Figure 2.10. Calculated daily maximum (a) and minimum (b) values of relative humidity

a)

b)

Figure 2.11. Calculated and measured daily maximum (a) and minimum (b) values of temperature from 2005 to 2007

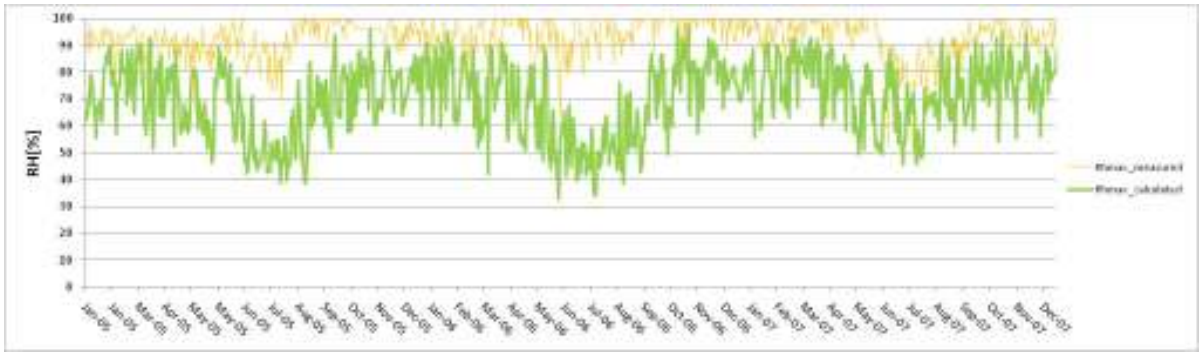

a)

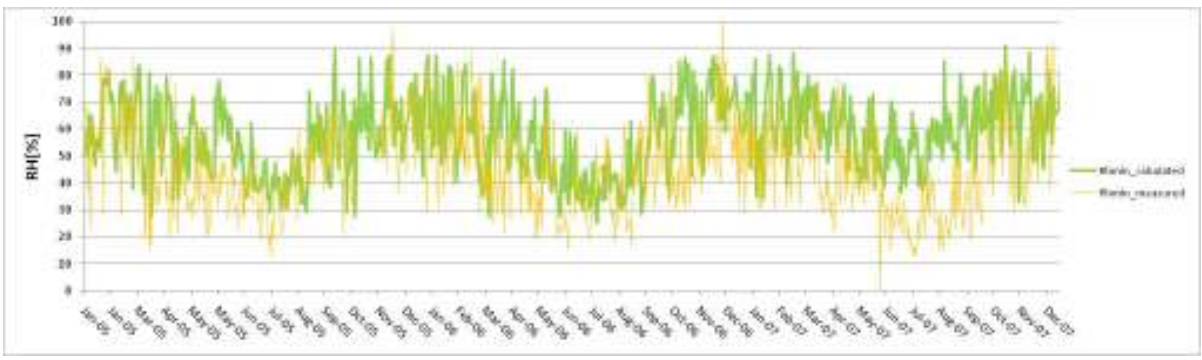

b)

Figure 2.12. Calculated daily maximum (a) and minimum (b) values of relative humidity from 2005 to 2007

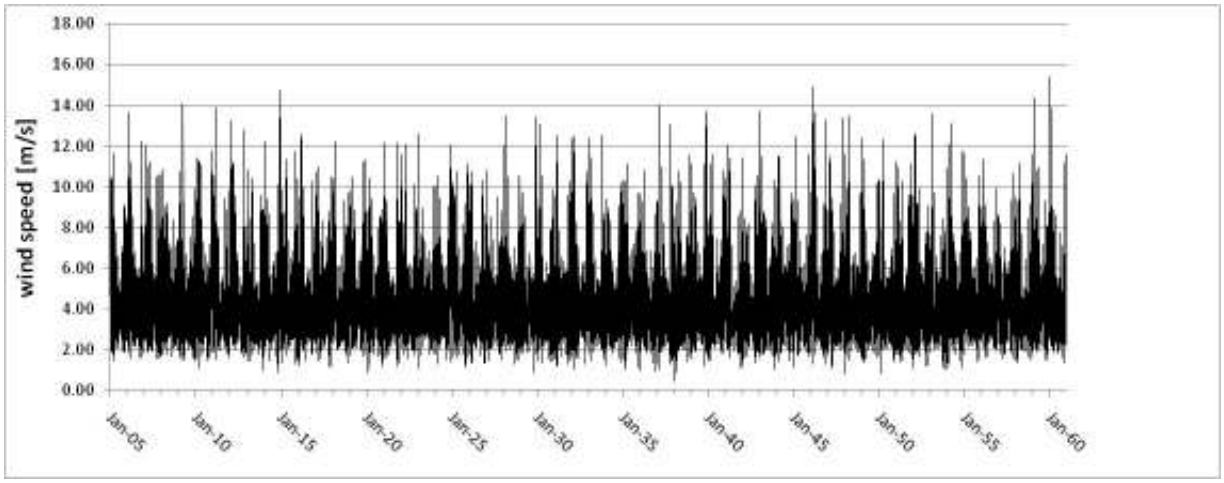

Figure 2.13. Calculated daily values of wind speed

3. The numerical model

3.1 Water and heat flow equations

VADOSE/W (Krahn, 2004) is a FEM code able to solve seepage problems within soils subjected to non-isothermal conditions established by seasonal climatic changes. Therefore, it is formulated to study the hydraulic flow (both water and vapour phases), the heat flow and the gas flow.
According to the assumptions adopted for our analyses
a) one- dimensional flow,
b) neglecting of gas flow,
c) neglecting of transpiration phenomena,
the problem is governed by mathematical equations that have to model the 1D hydraulic and heat flows.

The governing differential equation for one-dimensional vertical hydraulic seepage can be expressed as

$$m_w \frac{\partial u_w}{\partial t} = \frac{1}{\rho_w} \frac{\partial}{\partial y}\left(D_v \frac{\partial u_v}{\partial y} \right) + \frac{\partial}{\partial y}\left[k_{wy} \frac{\partial\left(y + \frac{u_w}{\rho_w g} \right)}{\partial y} \right] + Q_w \qquad [3.1]$$

where
- u_w = water pressure of soil moisture;
- u_v = vapour pressure of soil moisture;
- m_w = slope of the volumetric water content function;
- ρ_w = density of water;
- t = time;

- y = elevation head;
- D_v = vapour diffusion coefficient;
- k_{wy} = hydraulic conductivity in the vertical y-direction;
- g = gravity acceleration;
- Q_w = applied hydraulic boundary flux.

At the same time, the heat transfer is governed by:

$$\lambda_t \frac{\partial T}{\partial t} = \frac{\partial}{\partial y}\left(k_{t,y} \frac{\partial T}{\partial y} \right) + \rho c V_y \frac{\partial T}{\partial y} + L_v \frac{\partial}{\partial y}\left(D_v \frac{\partial u_v}{\partial y} \right) + Q_t \qquad [3.2]$$

where

- T = temperature;
- λ_t = volumetric heat capacity of soil;
- k_{ty} = thermal conductivity in the vertical y-direction;
- ρ = bulk density of soil;
- c = mass specific heat capacity of soil;
- V_y = Darcy water velocity in vertical y-direction;
- L_V = latent heat of vaporization of water;
- Q_t = applied thermal boundary flux.

The equations [3.1] and [3.2], which state that the difference during time between the flow entering and leaving an elemental volume at a point is equal to the rate of change of the volumetric water or heat contents with respect to time, contain three unknown parameters:
1) pore-water pressure u_w;
2) pore-vapour pressure u_v
3) temperature T.
The solution of the problem evidently needs the use of a third equation that couples heat and mass equations. The code uses the one proposed by Edlefsen and Anderson (1943),

$$u_v = u_{vs} \cdot \exp\left(\frac{-u_w w}{\rho R T} \right) = u_{vs} \cdot h_{r,air} \qquad [3.3]$$

where
- u_{vs} = saturated vapour pressure of pure free water;
- w = molecular mass of water vapour;
- R = universal gas constant;
- $h_{r,air}$ = relative humidity of air

3.2 Climate boundary conditions

As known, the solution of differential equations depends on the imposition of correct boundary conditions. In particular for our case, the most considerable variables to quantify are the magnitude of surface infiltration and actual evaporation. With regard to this topic, VADOSE/W evaluates the surface boundary conditions by coupling the moisture and heat stress states at the ground surface with climate conditions acting above the ground surface.

In order to obtain the atmospheric coupling, the code calculates the soil evaporative flux based on the Penman-Wilson equation (1990)

$$AE = \frac{\Gamma Q + \upsilon E_a}{\upsilon A + \Gamma} \qquad [3.4]$$

where

- AE = actual vertical evaporative flux from soil surface;
- Γ = slope of the $u_{vs} - T$ curve (saturated vapour pressure – temperature);
- Q = net radiant energy available at the soil surface;
- υ = psycrometric constant;
- $E_a = f(u) \cdot P_a \cdot (B - A)$
- $f(u) = 0.35\ (1+0.15\ U_a)$, function dependent on wind speed, surface roughness and eddy diffusion;
- U_a = wind speed;
- P_a = vapour pressure in the air above the evaporating surface;
- $B = 1/\ h_{r,air}$, inverse of the relative humidity of the air;
- $A = 1/h_r$, inverse of the relative humidity of the soil surface.

So doing, the equation [3.4] that calculates the actual evaporation AE needs data about net radiation, wind speed, relative umidity of air and relative umidity of soil surface.

The net radiation Q available at the soil surface is calculated by the program on the basis of the daily climate input data assigned at each time-step in terms of:

- maximum and minimum values of air temperature;
- maximum and minimum values of relative humidity of air;
- rainfall;
- average wind speed.

Daily step is the time-step used by us. In particular, the air temperature has been assumed to daily reach its minimum and maximum values respectively at sunrise and at noon. At the same time, the relative humidity of air has been assumed to daily reach its minimum and maximum values respectively at noon and at sunrise. Both the air temperature and the air relative humidity have been assumed to sinusoidally distribute between the sunrise and the sunset times. Regarding rainfall, its distribution is considered by the code as applied sinusoidally between the hours 00:00 and 24:00.

VADOSE/W uses the assigned climate data in order to estimate net solar radiation for the site, based on the assigned latitude (40° N in our case) and season as well as internally calculated ground surface albedo.

3.3 Properties of the soils

The deposit has been simulated through an indefinitely thick soil column (Fig. 3.1). The upper 1m thick layer is characterized by the presence of the top soil (that is directly in contact with atmospheric conditions), while the lower represents the Varicoloured Clay. In order to solve the equations [3.1] and [3.2], the code needs information about hydraulic and thermal properties of both soils. In particular, we have to assign the following hydraulic functions

- *hydraulic conductivity curve*, $k_w - u_w$ (hydraulic conductivity – pore-water pressure;
- *volumetric water content curve* θ_w - u_w (volumetric water content – pore-water pressure)

and the following thermal functions

- *thermal conductivity curve* k_t - θ_w (thermal conductivity - volumetric water content);
- *volumetric heat capacity function* λ_t - θ_w (volumetric heat capacity - volumetric water content).

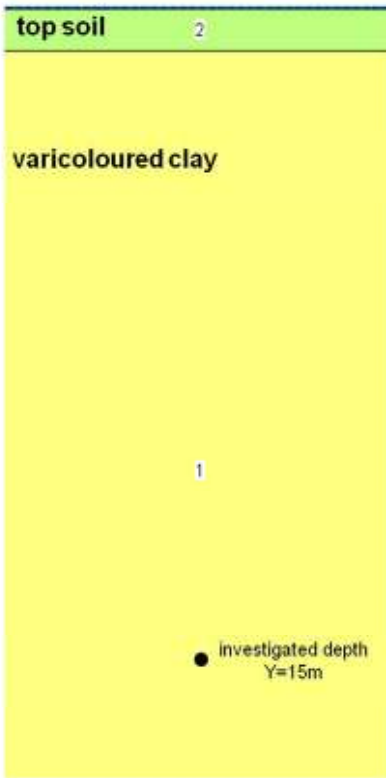

Figure 3.1. Scheme of the modelled soil column

Taking into account that the top soil has been considered essentially as a more pervious and more compressible soil than the clay, the assigned hydraulic and thermal properties are those having allowed in the analyses the best matching of the piezometric data measured at the depth Y = 15 m by the piezometer S1 between 01/01/2005 and 31/12/2007. In particular, the hydraulic conductivity curve of each soil (Fig. 3.2) has been derived as a function of matric suction u_a-u_w, using the formulation proposed by Mualem (1976)

$$k_w = \begin{cases} k_{ws} & \alpha \cdot (u_a - u_w) \le 1 \\ k_{ws} \cdot [\alpha \cdot (u_a - u_w)]^{-(2+5\lambda/2)} & \alpha \cdot (u_a - u_w) > 1 \end{cases} \quad [3.5]$$

where k_{ws} is the saturated permeability, a is the inverse of the air-entry suction $(u_a-u_w)_e$ and l is a dimensionless parameter representing the slope of the characteristic curve. Table 3.1 contains the parameters that have been used in the analyses.

Table 3.1. Hydraulic parameters assigned to the soils

	k_{ws} m/s	θ_{ws}	θ_{wr}	λ	α kPa^{-1}	a.e.v. kPa	Vol. Compress. m_{ws} (Sr=1) kPa^{-1}
Top soil	1,00E-05	0,40	0,00	0,50	0,100	10	1,00E-04
Varicoloured Clay	1,00E-08	0,40	0,00	0,50	0,014	70	1,00E-05

As regard the volumetric water content curve (Fig. 3.3), we have used the following formulation modified from Brooks and Corey (1964)

$$\theta_w = \begin{cases} \theta_{ws} - m_{ws} \cdot (u_a - u_w) & \alpha \cdot (u_a - u_w) \le 1 \\ \theta_{wr} + (\theta_{ws,aev} - \theta_{wr}) \cdot [\alpha \cdot (u_a - u_w)]^{-\lambda} & \alpha \cdot (u_a - u_w) > 1 \end{cases} \quad [3.6]$$

where θ_w is the volumetric water content (ratio of water volume to the total soil volume), θ_{ws} is the saturated volumetric water content (u_w=0), m_{ws} is the saturated volumetric compressibility of soil, θ_{wr} is the residual volumetric water content, $\theta_{ws,aev}$ represents the volumetric water content in correspondence of the air-entry value of the suction $(u_a-u_w)_e$, while a and l have the same previous significance (Tab. 3.1).

Thermal conductivity is defined as the quantity of heat that flows through a unit area of a soil of unit thickness in unit time under a unit temperature gradient, so it represents the ability of a soil to transmit heat by conduction. The units used in our analyses for thermal conductivity have been [kJ / (day m °C)]. The assigned function (Fig. 3.4) is the result of on estimation made by the code and derived from the Johansen method (1975), which is based on:

- the volumetric water content function;
- the thermal conductivity of the soil mineral.

In particular, the water content data is used to determine the range of possible water contents over which the thermal properties are defined. For both soils, the thermal conductivity of soil mineral has been imposed equal to 130 kJ / day m °C, which is typical of shales.

The volumetric heat capacity is instead defined as the quantity of heat required to raise the temperature of the soil by a unit degree. The units used in our analyses for heat capacity have been [kJ / m^3 °C]. For both soils, the function (Fig. 3.5) has been estimated by the method proposed by de Vries (1963), whose base of estimation is represented by:

- the volumetric water content function;
- the mass specific heat of the soil mineral.

In particular, the water content data is used to determine the range of possible water contents over which the thermal properties have to be defined. As regard the mass specific heat of the soil mineral, we have used for both soils the value 0.71 kJ / kg °C, which is suggested by the code as typical of soil minerals.

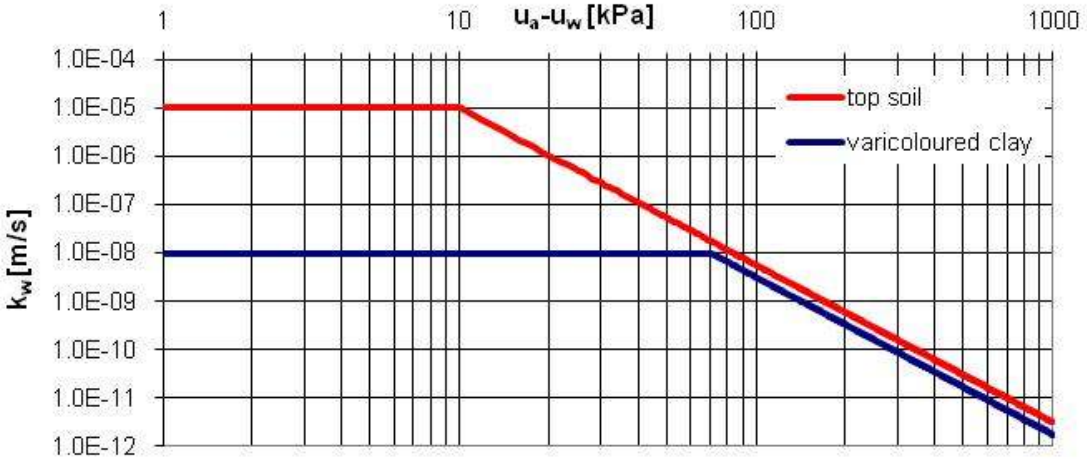

Figure 3.2. Hydraulic conductivity–suction curves used in the analyses

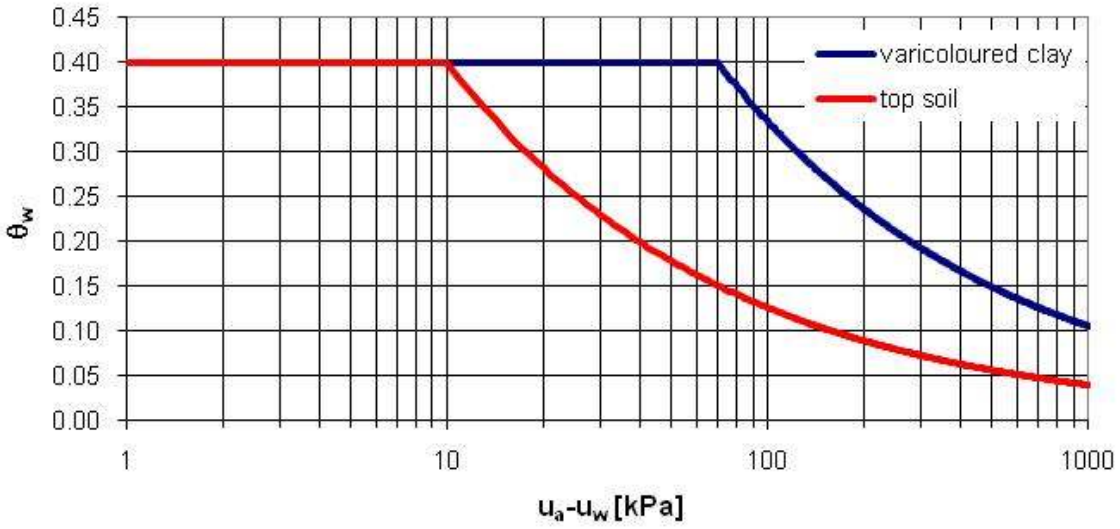

Figure 3.3. Volumetric water content-suction curves used in the analyses

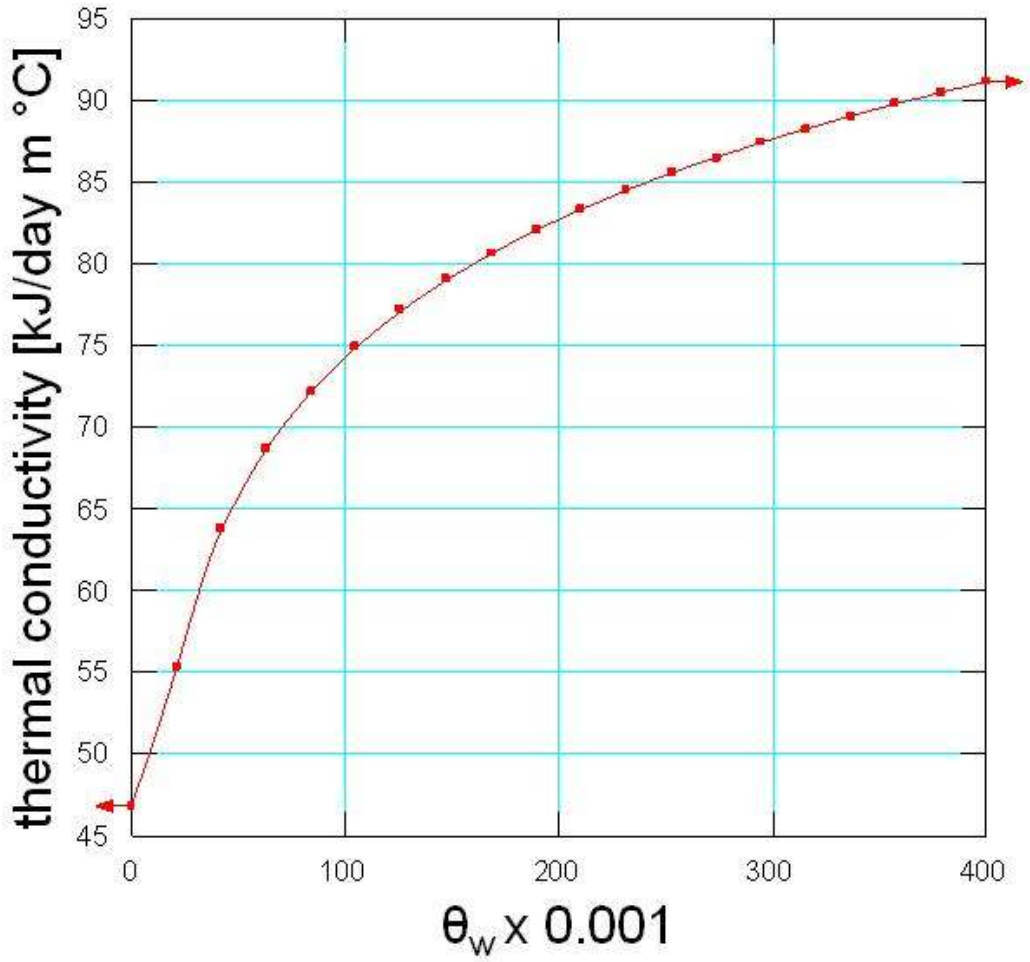

Figure 3.4. Thermal conductivity–volumetric water content curve used in the analyses

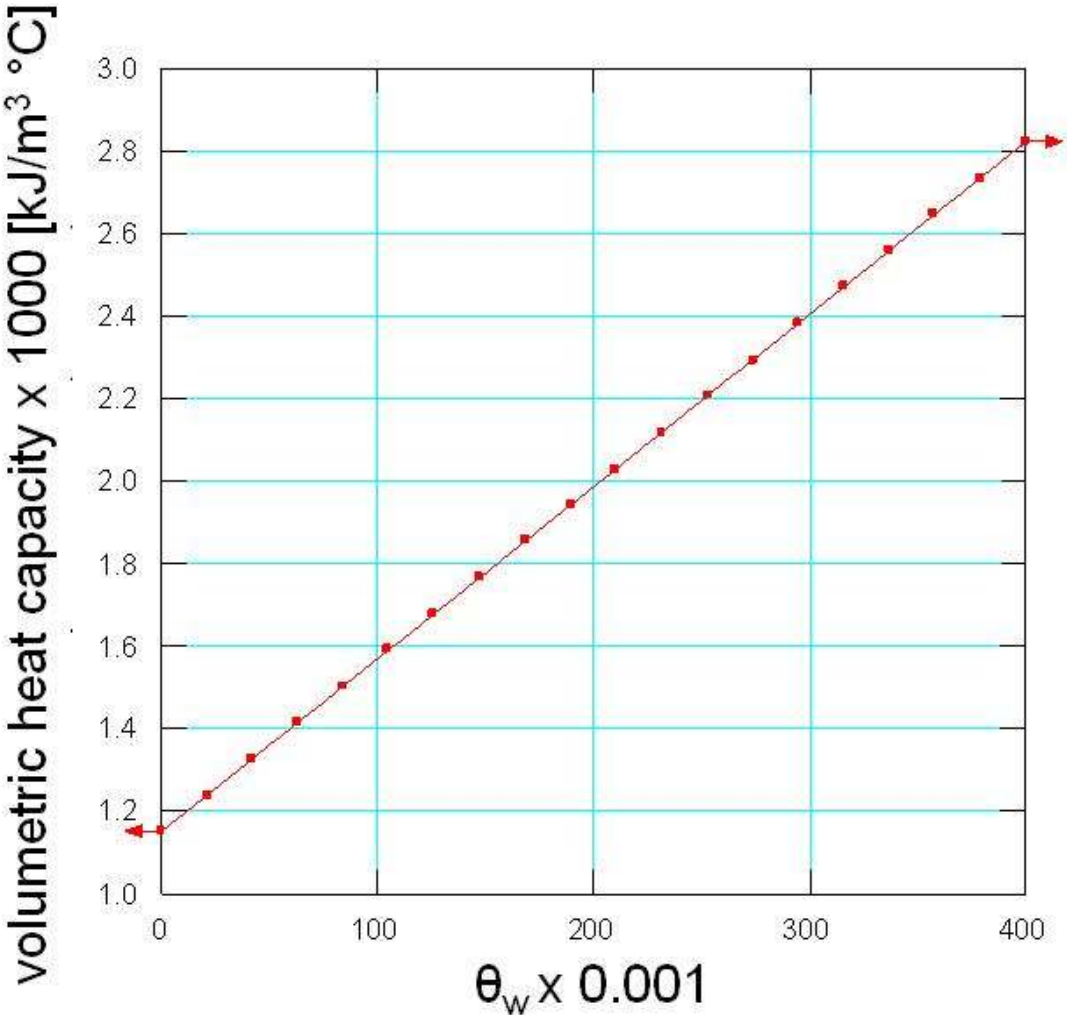

Figure 3.5. Volumetric heat capacity-volumetric water content curve used in the analyses

4. Results of the analyses

The first part of the analyses has concerned the calibration of the numerical model through the use of the data monitored during the three-year period 2005-2007.
After the calibration, we have performed some analyses aimed to define a long term scenario. In order to reach that goal, we have used as climatic boundary conditions the output data coming from the numerical analyses performed by the climatological task of C.I.R.A. through the use of the COSMO-CLM model.

4.1 Calibration of the numerical model

We have assigned at the ground surface the measured values reported in section 2.1 as climate boundary conditions. The analyses have been launched starting from the assigned initial conditions, that have consisted:

- in hydraulic terms, to input an hydrostatic condition with the groundwater set at the ground surface,
- in thermal terms, to input an initial temperature equal to 0°C at the ground surface.

The consequent piezometric course simulated by the analyses (Fig. 4.1a) is very similar to the measures. In particular the agreement is rather good after the first year (2005), which is probably more conditioned by the initial conditions. It's worth noting that the obtained result is the effect of a complex phenomena passing through the daily net infiltration furnished by the code as a result of the calculated net radiation and actual evaporation (Fig. 4.2a).

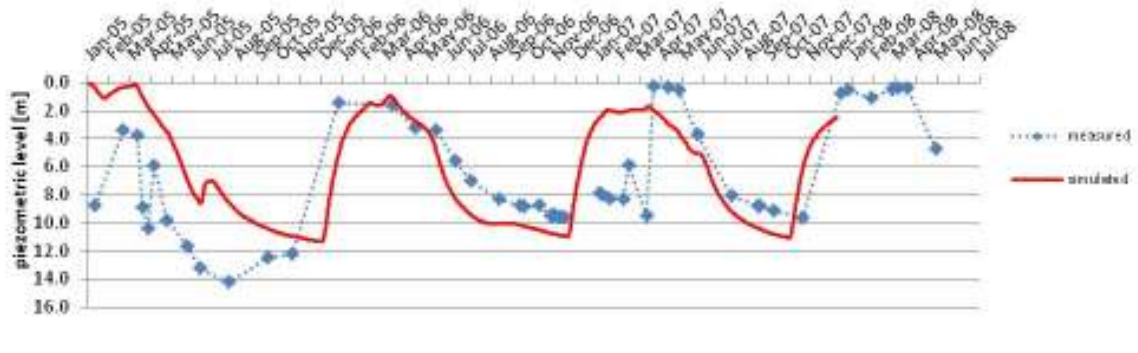

a)

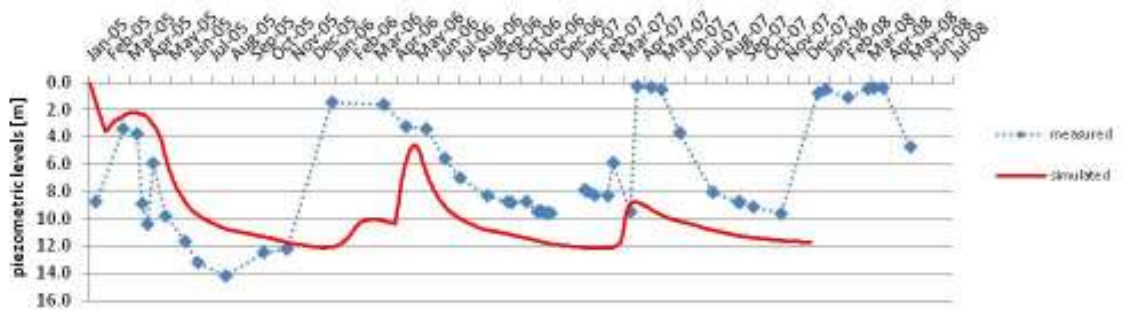

b)

Figure 4.1. Measured and simulated piezometric levels at the depth Y = 15 m. Boundary condition: a) measured climate data; b) calculated climate data

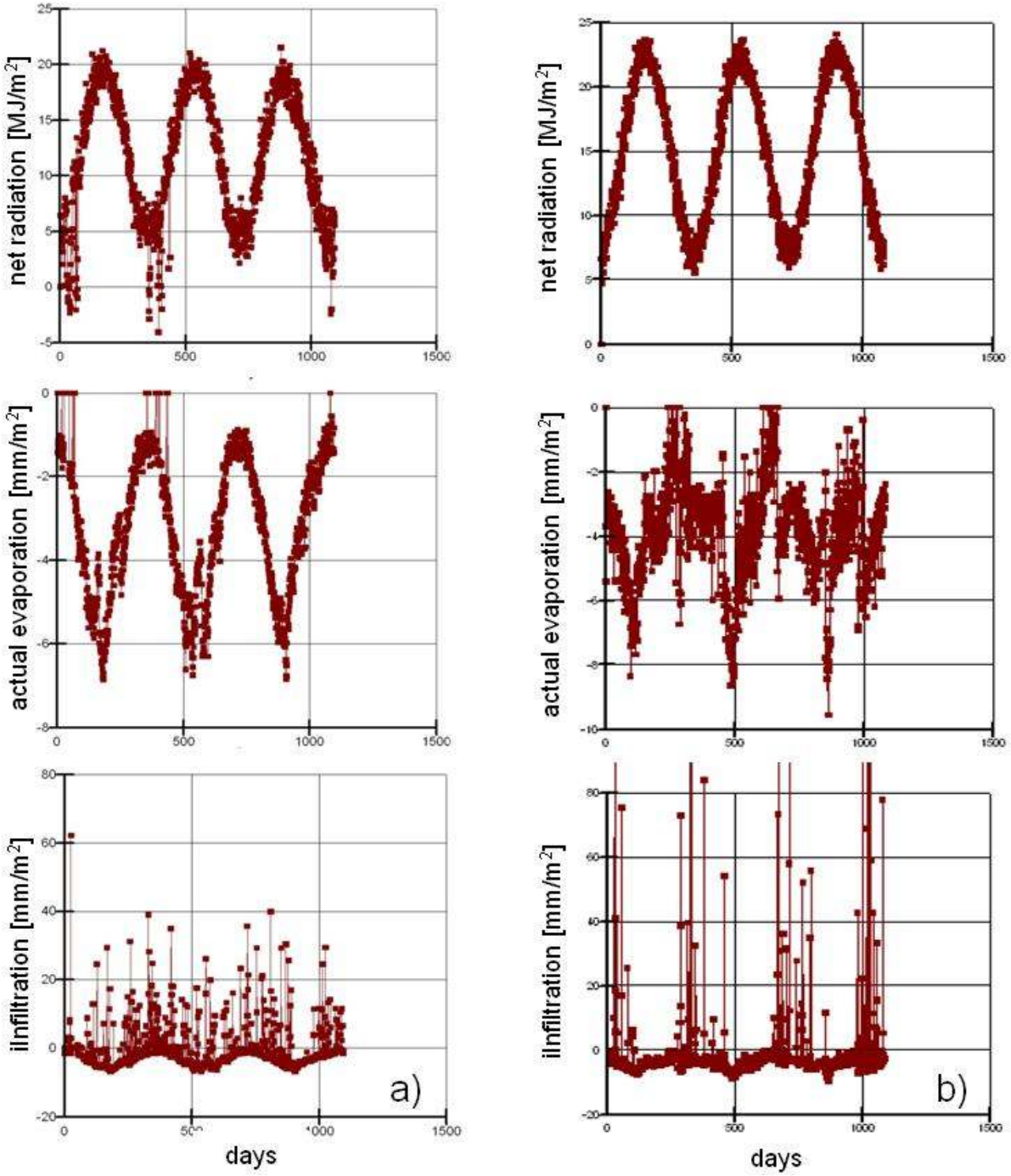

Figure 4.2. Calibration of the model: net radiation, actual evaporation and infiltration calculated by the code VADOSE/W. Boundary condition: a) measured climate data; b) calculated climate data

On the other hand, by the use of the calculated climate data (reported in section 2.2) as boundary condition, we have noted a worst correlation between the measured and simulated piezometric levels (Fig. 4.1b). Likely, this is essentially due to the fact that if compared with the evidence

- the calculated number of rainy days is very lower (Fig. 2.9b)

- the calculated values of minimum temperature are higher (Fig. 2.12b)
- the calculated values of maximum relative humidity are higher (Fig. 2.13a)

which contribute to reduce the daily infiltration (Fig. 4.2b) and consequently the piezometric levels.

Therefore, in order to obtain a more realistic future scenario, a statistical correction of the calculated climate data has been thought necessary.

4.1.1 Statistical correction of the calculated climate data

Because of the different distribution along the year shown by measures and calculations (Fig. 2.7), we firstly decided to calibrate only the daily rainfall according to the same daily distribution observed during 2006, but keeping for each year the value of the corresponding cumulated yearly rainfall (i.e. the same rate with respect to the yearly cumulated rainfall observed during 2006 has been assigned to each daily rainfall). We have chosen the year 2006, because we have noted that when we have operated this correction to measures (Fig. 4.3), we have obtained a fine correlation between simulated and measured piezometric level too (Fig. 4.4).

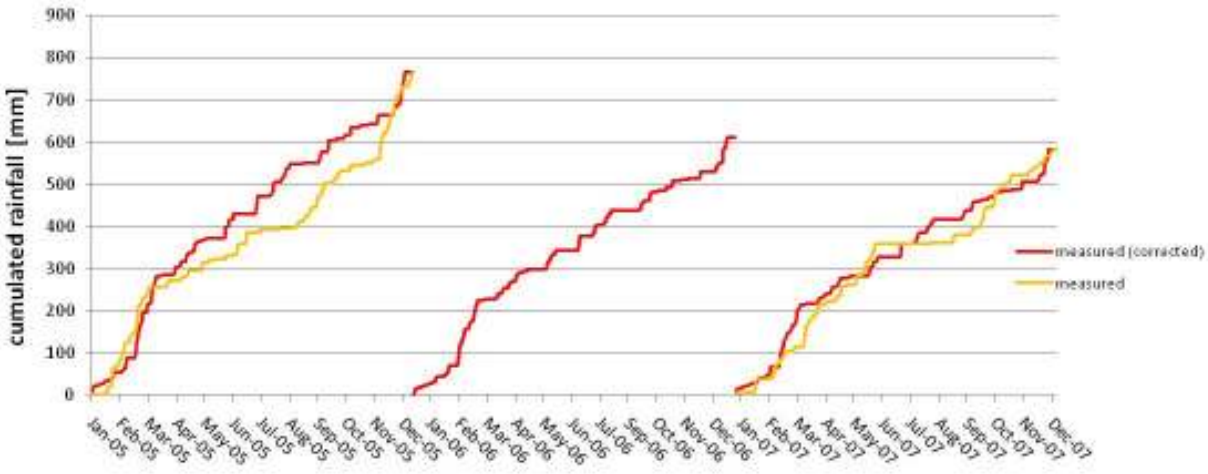

Figure 4.3. Correction of the measured daily rainfall

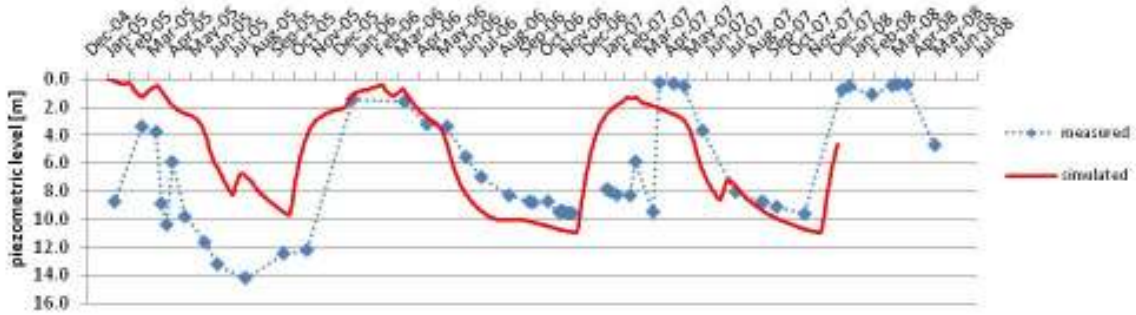

Figure 4.4. Measured and simulated piezometric levels at the depth Y = 15 m. Boundary condition: a) measured climate data (daily rainfall corrected)

Unfortunately, an equally fine correlation has not been obtained, simply by making that correction on the calculated daily rainfall (Fig. 4.5), as shown by Figure 4.6.

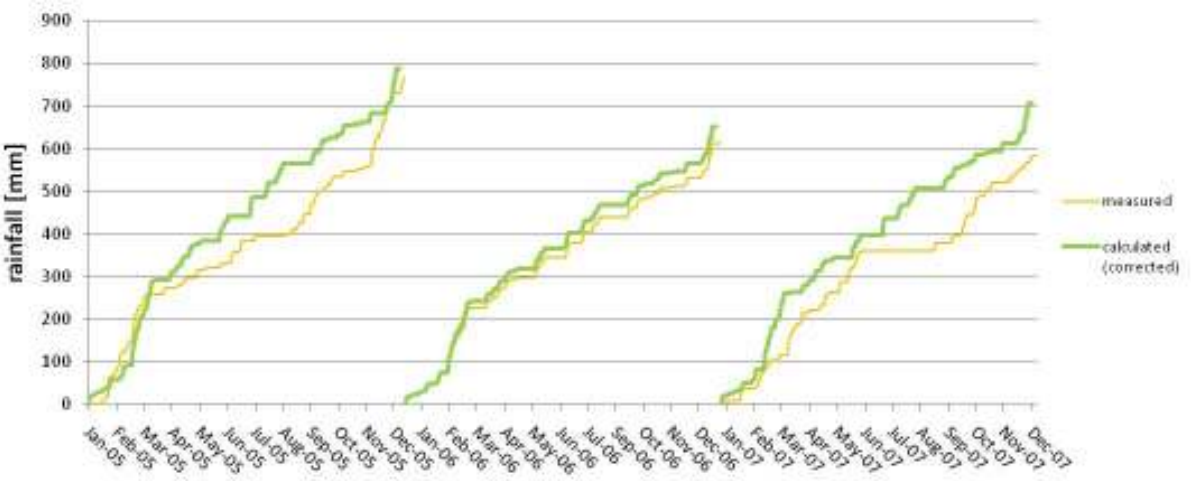

Figure 4.5. Correction of the calculated daily rainfall

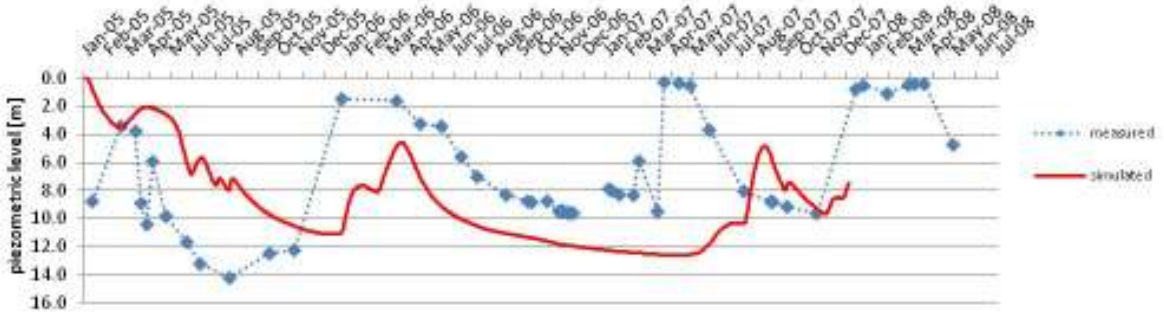

Figure 4.6. Measured and calculated piezometric levels at the depth Y = 15 m. Boundary condition: a) calculated climate data (only daily rainfall corrected)

Therefore, we decided to correct the other climate data too. In order to do that, we have used the “quantilebased” bias correction scheme (Wood et al., 2004), which essentially rescales the calculated data to match the observations. That correction occurs after a comparison between the simulated cumulative frequency distribution and the observed one: the simulated value is replaced by the observed value having the same percentile. This method is considered particularly efficient because it removes the median differences to zero.
In our case, the bias correction has been performed on the daily maximum and minimum values of temperature and relative humidity calculated and observed from 2005 to 2007 (Figs. 4.7 and 4.8). As we expected, the cumulative frequency curves of the calculated minimum values of temperature (Fig. 4.7b) and maximum values of relative humidity have shown (Fig. 4.8b) the highest differences compared to the corresponding observed cumulative frequency distribution. Using the bias corrected calculated climate data, reported by Figures 4.9 and 4.10, as input data (daily rainfall has been again corrected according to the distribution of 2006), we have obtained a substantially acceptable matching between observed and simulated pore-water

pressures (Fig. 4.11). Due to this positive statement of fact, we have decided to correct also the future climate data by using this technique, in order to outline a reliable future scenario.

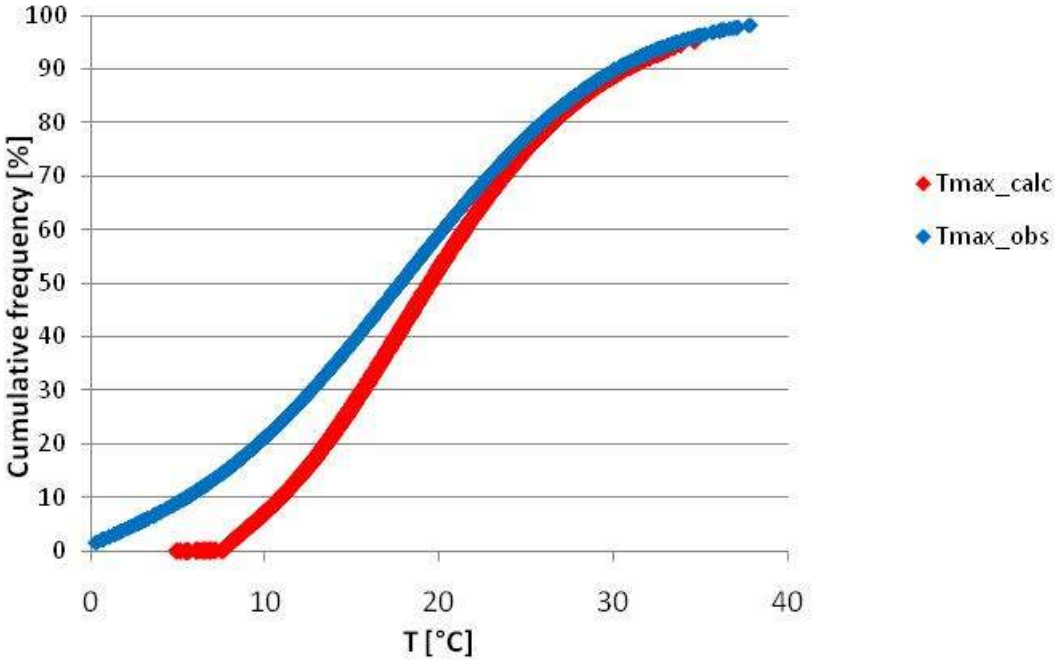

a)

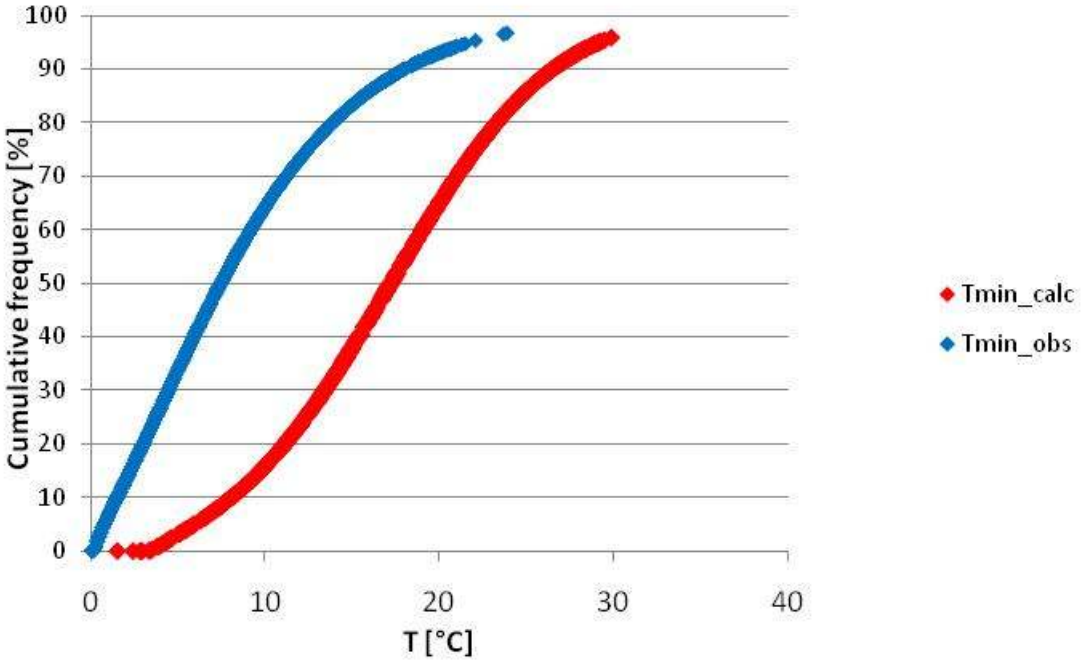

b)

Figure 4.7. Cumulative frequency curves of the observed and calculated daily maximum (a) and minimum (b) values of temperature T from 2005 to 2007

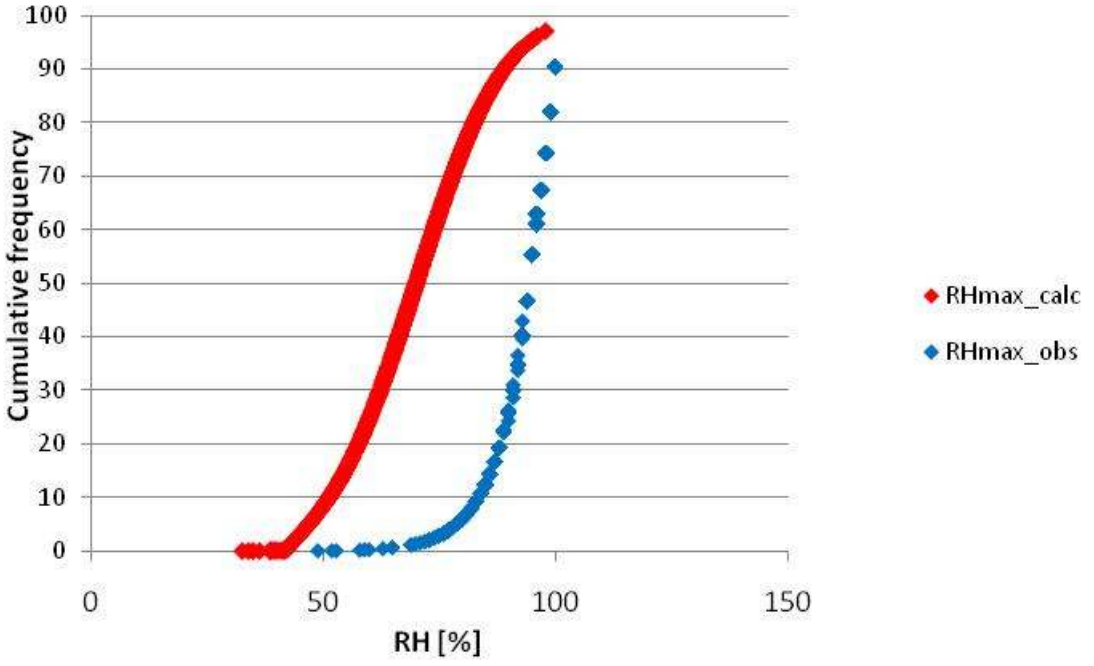

a)

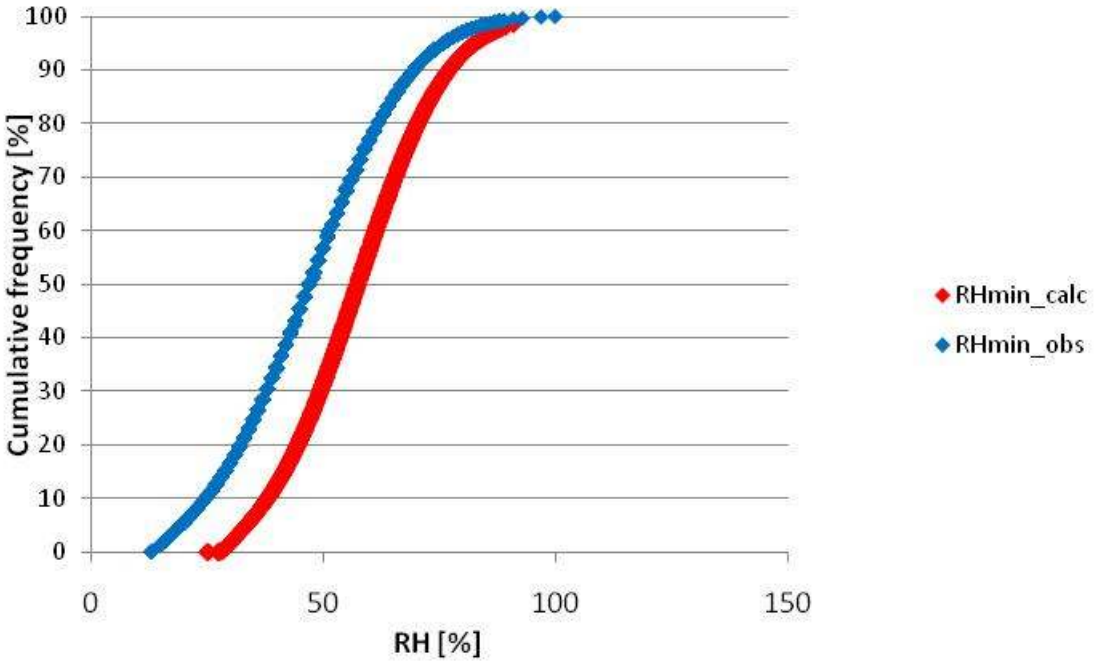

b)

Figure 4.8. Cumulative frequency curves of the observed and calculated daily maximum (a) and minimum (b) values of relative humidity RH from 2005 to 2007

a)

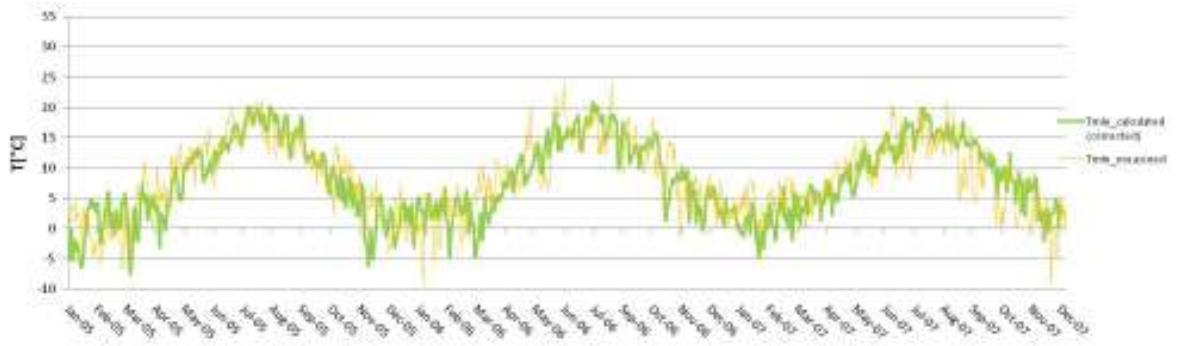

b)

Figure 4.9. Calculated (corrected) and measured daily maximum (a) and minimum (b) values of temperature from 2005 to 2007

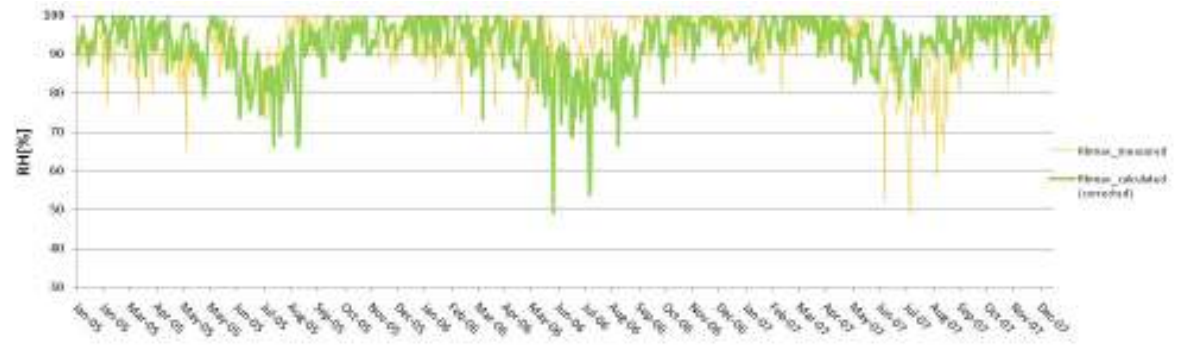

a)

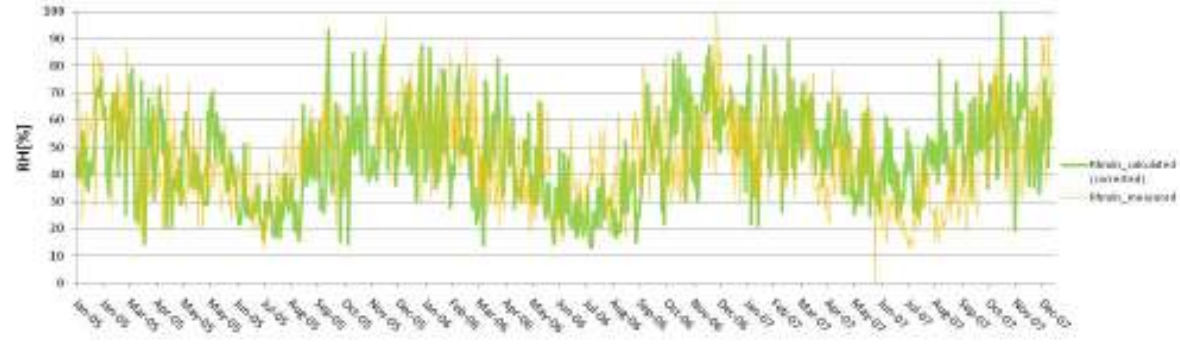

b)

Figure 4.10. Calculated (corrected) and measured daily maximum (a) and minimum (b) values of relative humidity from 2005 to 2007

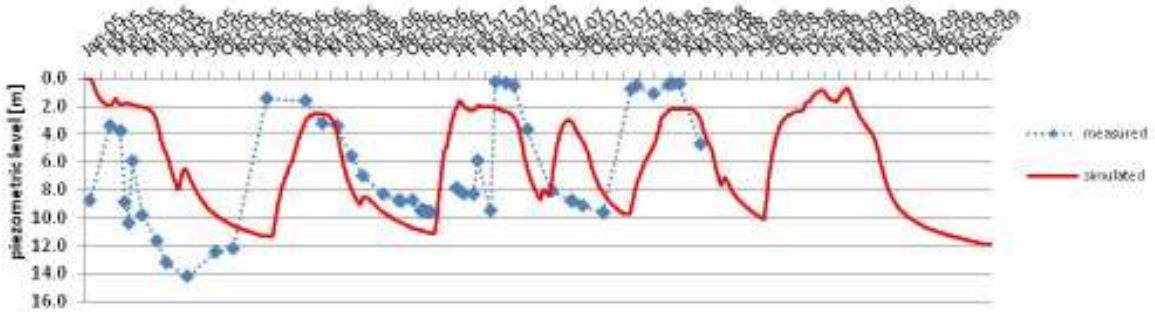

Figure 4.11. Measured and simulated piezometric levels at the depth Y = 15 m. Boundary condition: calculated climate data (corrected)

4.2 Estimation of a potential future scenario

Once calibrated the model, the future climate data calculated until 2060 (and opportunely corrected) have been used as boundary condition. The combination of the effects produced by

- yearly cumulated rainfall, which show a tendency to decrease on average with a gradient of about -1.80 mm/year (Fig. 2.8);
- maximum and minimum temperature, which show a tendency to increase on average with a gradient of about 0.03 °C /year (Fig. 4.12);
- maximum and minimum relative humidity, which show a tendency to decrease on average with a gradient of about -0.04 % /year (Fig. 4.13);

tend to favour evaporative effects and so to reduce the infiltration. Due to the combination of these effects, the future piezometric levels (Fig. 4.14), simulated by the seepage analyses, fluctuate showing a substantially slow reduction (about -4 cm/year).

The combination of these results with the already back analysed relationship [2.1] between daily pore-water pressures and velocity, has allowed also to furnish a scenario about the future rates of movements. In particular, according to our estimation, the mean velocity could reduce of about 0.02 cm/year (Fig. 4.15a), with acceleration in correspondence to the most rainy years (Fig. 4.15b).

Moreover, the Figure 4.16 shows the course of the displacements as a result of the integration of the calculated daily velocities: according to this estimation, the displacements cumulated during the next 50 years will attain a value lower than 1.00 m.

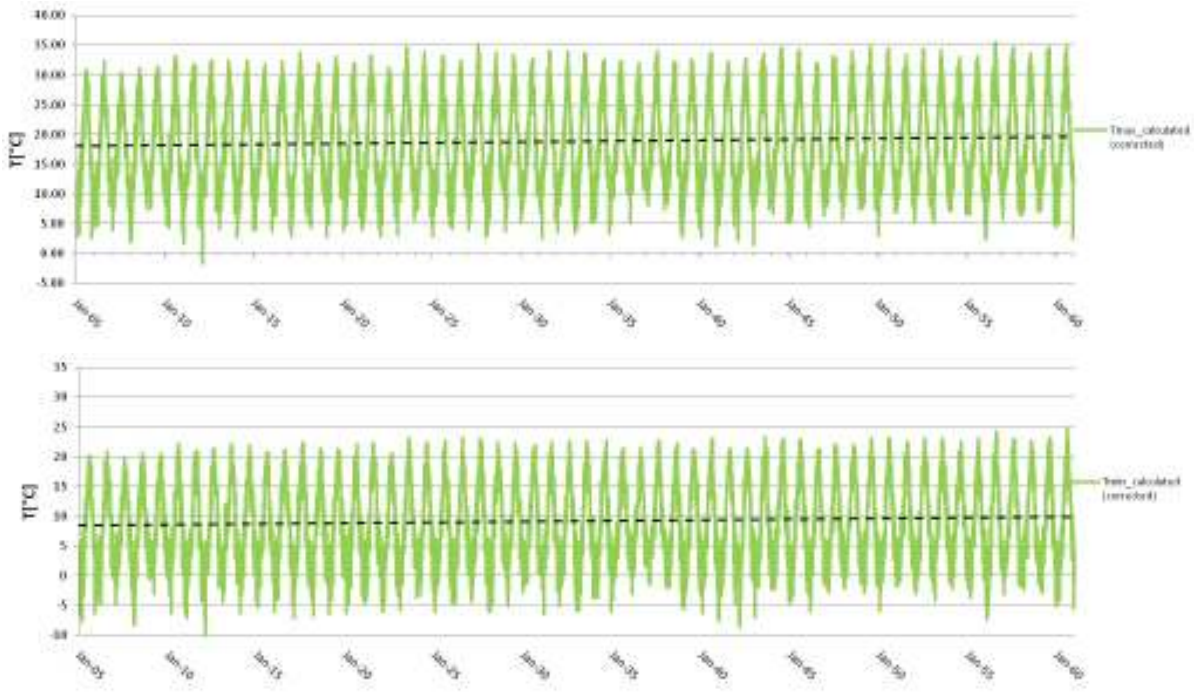

a)

b)

Figure 4.12. Calculated (corrected) future daily maximum (a) and minimum (b) values of temperature

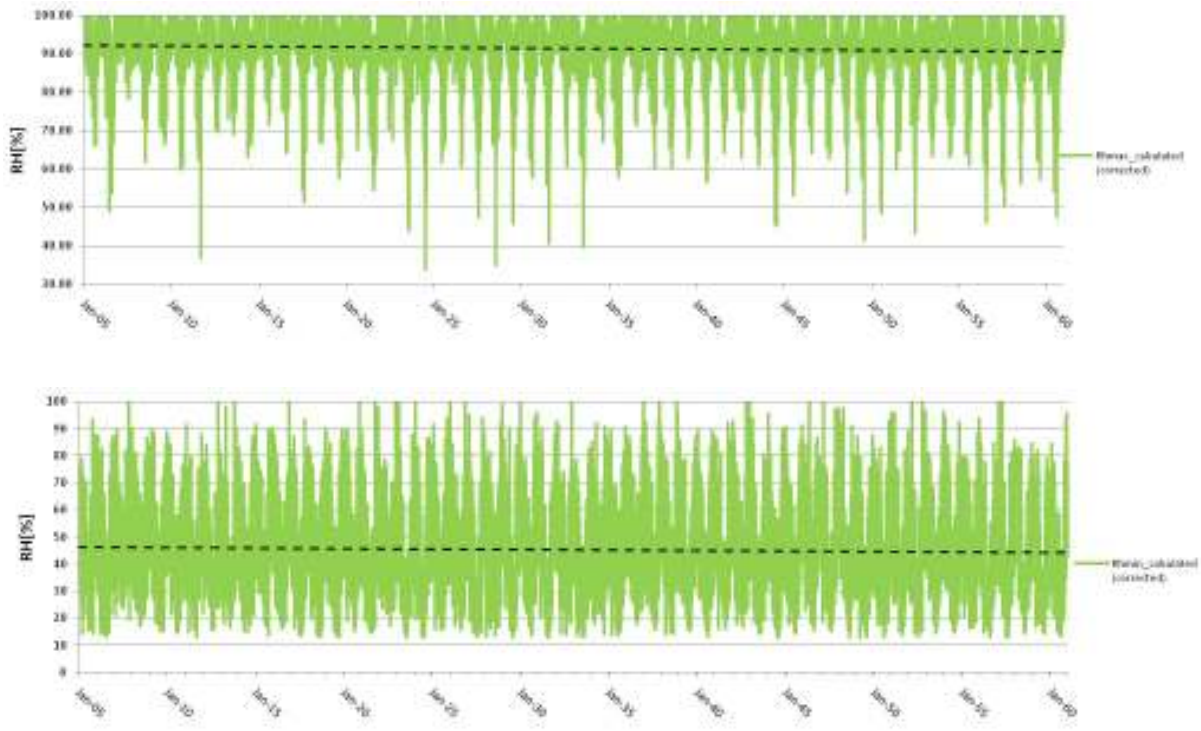

a)

b)

Figure 4.13. Calculated (corrected) future daily maximum (a) and minimum (b) values of relative humidity

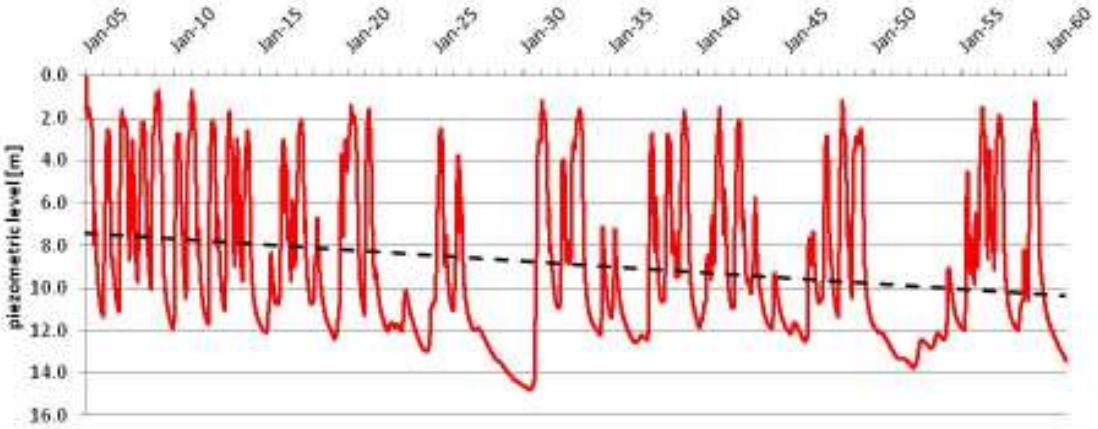

Figure 4.14. Calculated future daily piezometric level maximum (a) and minimum (b) values of relative humidity

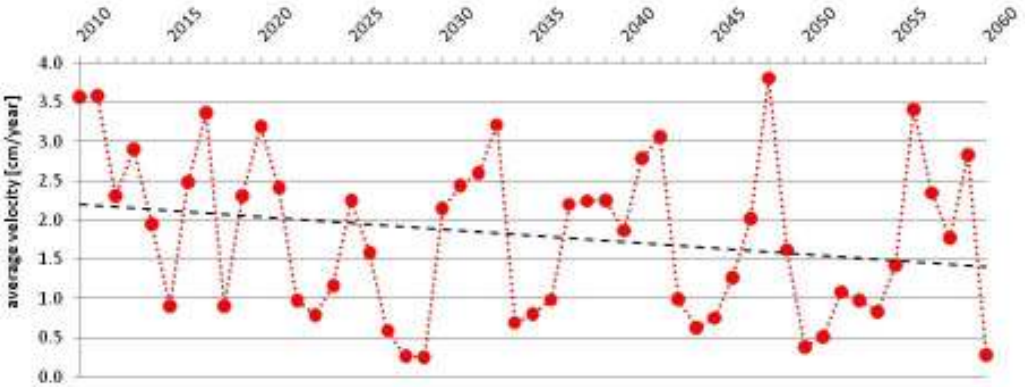

a)

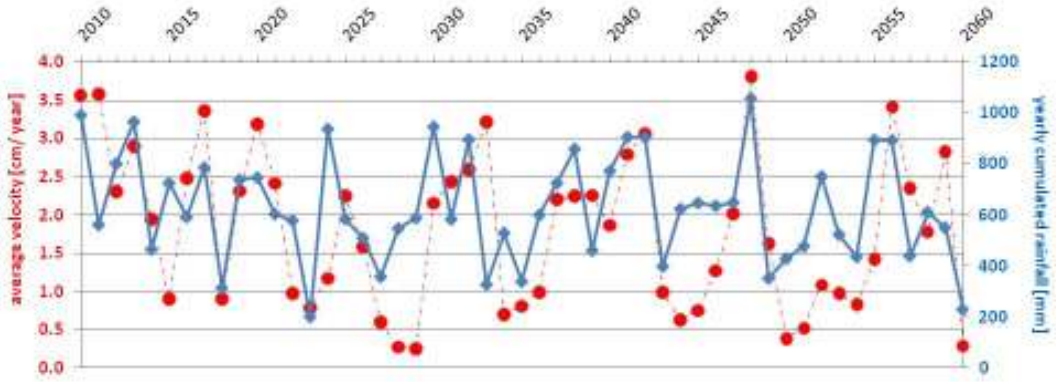

b)

Figure 4.15. Estimated future main rate of movement

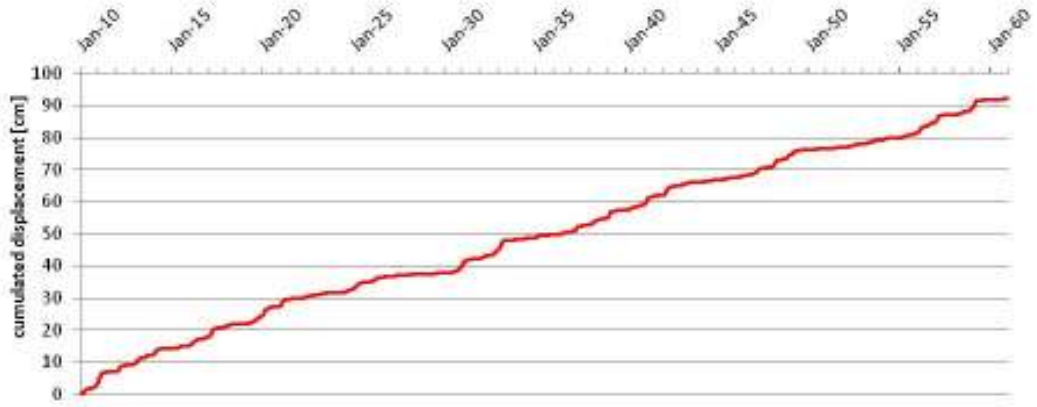

Figure 4.16. Estimated future cumulated displacements

5. Conclusive remarks

An evaluation of the influence of the clime on the behaviour of a slow landslide in clay has been the object of this Technical Report. Due to the low hydraulic conductivity of the involved soils that reduce the infiltration, the activity of this kind of landslide is generally not conditioned by single intense rainy events, but, on the contrary, is normally governed by the rainfall cumulated over long time periods.

We propose a methodological approach aimed to link climate data to movements and consisting in two fundamental steps

a) individuation of a correlation between monitored climatic data and monitored piezometric regime;
b) individuation of a relationship between monitored piezometric regime and monitored displacements within the track of an active earthflow

In order to reach the first goal, a 1D numerical simulation of the infiltration within a soil subjected to the non-isothermal conditions established by seasonal climatic changes has been implemented through the use of the FEM code VADOSE/W. These analyses have allowed to reproduce the course of the pore-water pressure monitored within the landslide body during a three-year period. The hydraulic and thermal properties assigned to the involved soils have been chosen in order to have the best matching of the observed values. The second goal has been achieved through the definition of an opportunely back-analyzed relation between observed piezometric regime and rates of movements.

Once calibrated the infiltration model, we have tried to provide an estimation of the long-term behaviour of the analyzed landslide, taking into account the indications about the climate scenario for the next 50 years. Those indications, which have been derived from the results of the numerical analyses coming from the climatologic model COSMO-CLM and performed by the climatologic task of C.I.R.A., highlight some aspects of the climate change as

- decreasing tendency of the yearly cumulated rainfall;

- increasing tendency of the temperature;
- decreasing tendency of the relative humidity.

The combination of these climate trends produce the reliable effect of favouring evaporation and so of reducing infiltration. According to our results, these phenomena should produce a future reduction of the piezometric levels, and first of all, as a macroscopic effect, the overall slowing down of the movements.

6. *References*

Brooks R.H., Corey A.T. (1964). Hydraulic properties of porous media. Hydrology Paper No.3, Colorado State Univ., Fort Collins, Colorado

Cruden D.M., Varnes D.J. (1996). Landslides Types and Processes. In: Turner A.K. & Schuster R.L. (Eds.) Landslides: Investigation and Mitigation. Transportation Research Board Special Report 247. National Academy Press, WA, 36-75

de Vries D.A. (1963). Thermal properties of soils. p. 210–235. In W.R. Van Wijk (ed.) Physics of plant environment. North-Holland Publ. Co., Amsterdam

Johansen O. (1975). Thermal conductivity of soils. Ph.D. diss. Norwegian Univ. of Science and Technol., Trondheim (CRREL draft transl. 637, 1977)

Krahn J. (2004). Vadose Zone Modeling with VADOSE /W – An Engineering Methodology. GEO-SLOPE International Ltd., Calgary, Canada

Mualem Y. (1976). A new model for predicting the hydraulic conductivity of unsaturated porous media. Water Resources Research, 12, pp. 513-522

Vassallo R., Di Maio C. (2006). La frana di Costa della Gaveta a Potenza: analisi preliminare. Incontro Annuale dei Ricercatori di Geotecnica, Pisa, Giugno 2006.

Vassallo R., Di Maio C. (2007). La frana di Costa della Gaveta a Potenza. Incontro Annuale dei Ricercatori di Geotecnica, Salerno, Luglio 2007.

Vassallo R., Di Maio C. (2008). Misure di spostamenti superficiali e profondi in un versante argilloso in frana. Incontro Annuale dei Ricercatori di Geotecnica, Catania, Settembre 2008.

Wood A.W., Leung L.R., Sridhar V., Lettenmaier D.P. (2004). Hydrologic implications of dynamical and statistical approaches to downscale climate model outputs, Clim. Change, 62, 189-216